

PositionIC: Unified Position and Identity Consistency for Image Customization

Junjie Hu^{1,2,*} Tianyang Han^{1,*} Kai Ma^{1,†} Jialin Gao¹ Song Yang¹ Xianhua He¹
 Junfeng Luo¹ Xiaoming Wei¹ Wenqiang Zhang^{2,3}

¹MeiGen AI Team, Meituan

²Shanghai Key Lab of Intelligent Information Processing,

College of Computer Science and Artificial Intelligence, Fudan University, Shanghai, China

³College of Intelligent Robotics and Advanced Manufacturing, Fudan University, Shanghai, China

Abstract

Recent subject-driven image customization excels in fidelity, yet fine-grained instance-level spatial control remains an elusive challenge, hindering real-world applications. This limitation stems from two factors: a scarcity of scalable, position-annotated datasets, and the entanglement of identity and layout by global attention mechanisms. To this end, we introduce PositionIC, a unified framework for high-fidelity, spatially controllable multi-subject customization. First, we present BMPDS, the first automatic data-synthesis pipeline for position-annotated multi-subject datasets, effectively providing crucial spatial supervision. Second, we design a lightweight, layout-aware diffusion framework that integrates a novel visibility-aware attention mechanism. This mechanism explicitly models spatial relationships via an NeRF-inspired volumetric weight regulation to effectively decouple instance-level spatial embeddings from semantic identity features, enabling precise, occlusion-aware placement of multiple subjects. Extensive experiments demonstrate PositionIC achieves state-of-the-art performance on public benchmarks, setting new records for spatial precision and identity consistency. Our work represents a significant step towards truly controllable, high-fidelity image customization in multi-entity scenarios. Code and data: <https://github.com/MeiGen-AI/PositionIC>.

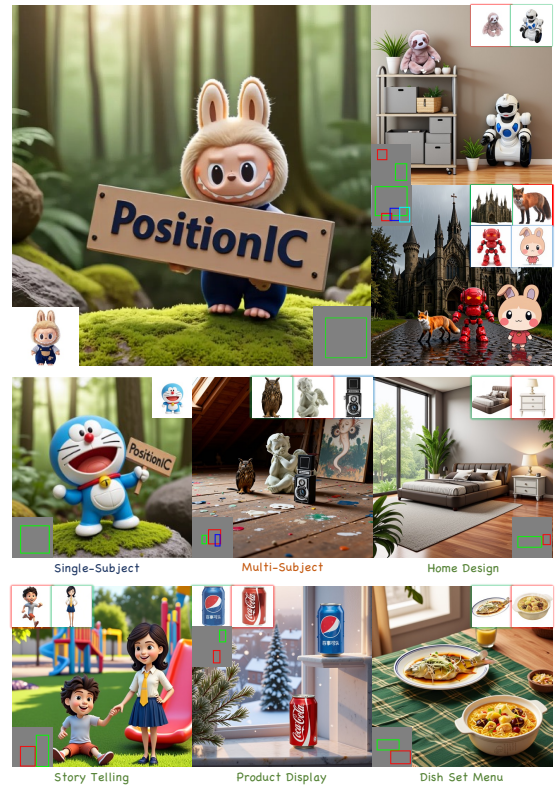


Figure 1. Results from PositionIC across various controllable image customization tasks.

1. Introduction

Diffusion-based models have recently revolutionized visual synthesis, especially in text-to-image (T2I) generation, where they produce photorealistic images closely aligned with short textual prompts [5, 14, 17, 23, 25]. Beyond generic generation, subject-driven image customization aims to integrate one or more reference objects into

user-specified scenes under the guidance of a text prompt. Traditionally, this task emphasizes two core goals: (i) preserving the appearance identity of the reference object(s), and (ii) aligning the synthesis with the user’s textual description, where remarkable improvements in visual fidelity have been achieved by recent methods [21, 28, 30, 35].

However, through exploring real-world applications like e-commerce product display, storybook illustration, and interior design, we identified an additional critical dimen-

*Equal Contribution.

†Project Leader.

sion: fine-grained, flexible spatial control, encompassing aspects such as subject placement, scale, occlusion, and relative layout. In other words, while prior works focus on “*what*” to generate, practical usage demands *where* and *how* each subject appears. To explicitly address this, we adopt a refined task definition: subject-driven customization with both identity fidelity and instance-level spatial controllability. This is a natural extension of the established task, not a fundamentally different objective, but one that better matches application requirements.

Despite substantial progress in identity-preserving personalization methods, current approaches still struggle with flexible placement and layout control. Specifically, two coupled bottlenecks remain: (1) the scarcity of large-scale datasets annotated with explicit positional labels of multiple subjects, hindering the learning of spatial reasoning; and (2) the prevalent use of global-level attention mechanisms in diffusion transformers, which inadvertently entangle semantic identity and spatial layout, thereby failing to provide fine-grained, visibility-aware control. While a few recent works [18, 33] have attempted layout control, they typically exhibit a trade-off between spatial precision and subject identity consistency, thus limiting their practical utility.

To this end, we introduce two tightly coupled components: (i) a scalable Bidirectional Multi-dimensional Perception Data Synthesis (BMPDS) pipeline that generates high-quality, multi-subject, position-annotated data; and (ii) PositionIC, a lightweight layout-aware diffusion framework incorporating a visibility-aware attention mechanism that enables precise, controllable placement of multiple subjects while maintaining identity fidelity.

Specifically, to overcome the data bottleneck, we devise an automatic pipeline that expands single-subject collections into scalable, high-quality multi-subject datasets annotated with explicit position masks. A hierarchical training schedule establishes a bidirectional generation paradigm, progressively moving from single-to-multi subject synthesis and back, so that resolution constraints are relaxed while subject drift is suppressed. Because of the inherent hallucination of Multi-modal Large Language Models (MLLMs) [7, 22], we avoid direct visual comparisons: expert vision models first translate visual content into textual descriptions, after which MLLMs perform multi-dimensional consistency checks. This two-stage filtering markedly improves data reliability.

Built upon the BMPDS corpus, PositionIC directly integrates our visibility-aware attention mechanism into the diffusion transformer architecture. This mechanism is achieved mainly via an operation inspired by NeRF [20] termed Volumetric Weight Regulation, which explicitly constructs attention masks based on the likelihood of visibility derived from volumetric rendering principles. Unlike prevalent global-level attention, our visibility-aware atten-

tion mechanism effectively decouples instance-level spatial embeddings from semantic identity features. This design enables independent and accurate placement of each subject by explicitly modeling occlusion and perspective relationships, and crucially introduces no extra train-time parameters or inference overhead. Restricting reference features to user-specified regions further enhances identity fidelity and spatial precision, unlocking new applications of controllable image customization (Figure 1).

Our contributions are summarized as follows:

- We present BMPDS, the first large-scale automatic data-synthesis framework for high-fidelity, position-annotated multi-subject pairs, filling a critical gap in spatial supervision.
- We propose PositionIC, a lightweight yet highly effective layout-aware diffusion framework. It integrates a novel visibility-aware attention mechanism into the diffusion transformer architecture. This design explicitly decouples spatial layout from semantic identity, enabling unprecedentedly accurate multi-subject placement and occlusion-aware rendering without additional training parameters or inference overhead.
- Extensive experimental results demonstrate that our approach delivers state-of-the-art performance on subject-driven customization benchmarks, achieving the highest spatial precision and identity consistency to date.

2. Related Work

2.1. Subject-driven Generation

In addition to using text prompts for conditional image generation, current diffusion models [1, 6, 10, 16, 34, 36, 38, 39] support reference image input to achieve preservation of subject identity. Dreambooth [26] and LoRa [9] control the generation of diffusion models through fine-tuning on the specific subject. Recently, Diffusion-Transformers-based subject-driven models [15, 21, 28, 29, 35, 37] further advance subject-driven generation. They introduce reference images as context information through token concatenation to ensure the consistency of objects during generation.

2.2. Position Controllable Generation

Some works [1, 4, 12, 27, 31, 32, 40] have attempted to generate with precise layout control. Gligen [18] encodes Fourier embedding as grounding tokens to inject position information. MS-diffusion [33] utilizes a grounding resampler correlating visual information with specific entities and spatial constraints. However, they still suffer from inconsistencies in vision and position, which hinder further application.

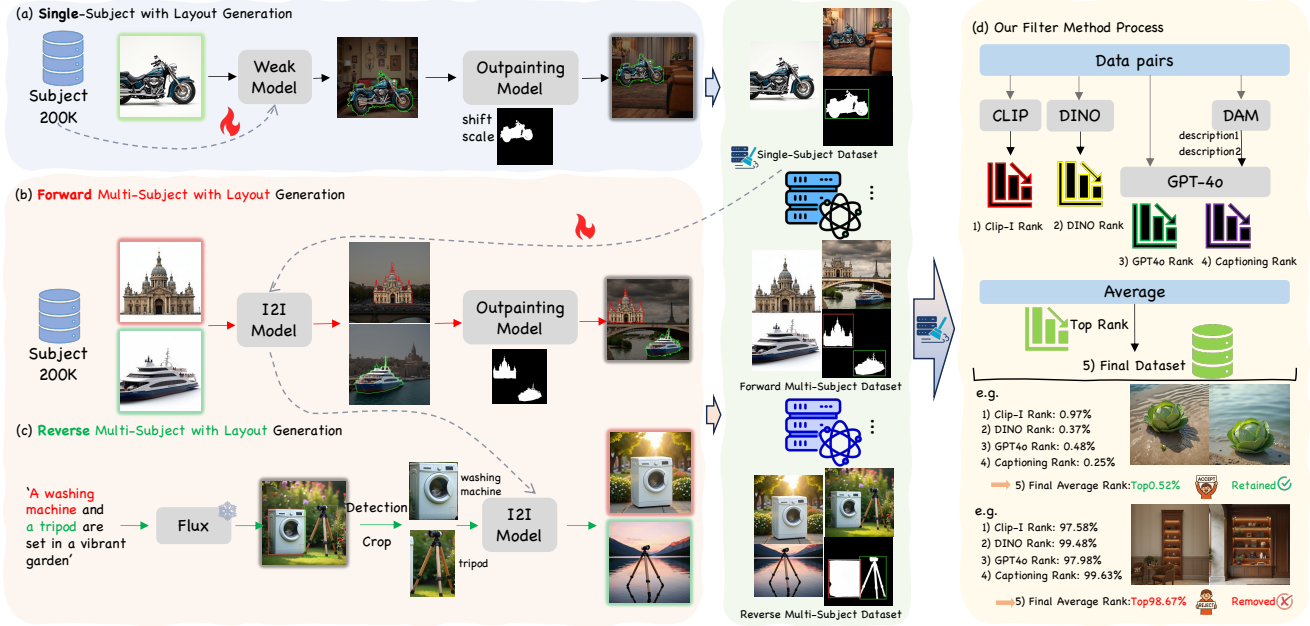


Figure 2. Bidirectional Multi-dimensional Perception Data Synthesis framework. (a) We use Subject200K to train a weak model. (b) Forward generation of multi-subject data pairs. (c) Reverse generation of multi-subject data pairs. (d) We utilize MLLMs to filter out our data pairs.

3. Method

3.1. Bidirectional Multi-dimensional Perception Data Synthesis (BMPDS)

Position-controllable image-driven customization requires high-fidelity paired data, featuring prominent subjects and high resolution with layout control signals. However, existing open-source datasets such as Subject200K [28] generate paired data using diptych images, which leads to object inconsistency issues and are limited by low resolution and the lack of positional information. We introduce **BMPDS**, a Bidirectional Multi-dimensional Perception Data Synthesis framework to tackle these limitations. We adopt a hierarchical generation-and-selection strategy to progressively improve data quality, gradually introducing single-image and multi-image pairs with spatial control information during generation. The overall framework is depicted in Figure 2.

3.1.1. Customized Data Paired Synthesis

We divide the automated data generation process into three stages. (1) Inspired by UNO, we first train a weak model for image customization tasks using Subject200K dataset. The generated results are then segmented and passed through a Flux-Outpainting model with random placement to inject spatial control information. The paired data obtained in this stage is filtered by a filter to ensure high fidelity. These data are then used to train the PositionIC-Single model. (2) In the second stage, we perform forward gen-

eration of multi-image data pairs. We independently process Subject200K samples via PositionIC-Single, then randomly pair the output and position the output as input to the Flux-Outpainting model, thereby obtaining multi-subject paired data. (3) To enhance data diversity and improve generalization, we reverse the above process in the third stage. We first use Large Language Models (LLMs) to generate text descriptions containing multiple subjects, then employ the Flux model to create high-resolution images. Objects are detected and cropped from these results, individually processed by the PositionIC-Single, resulting in high-resolution multi-subject paired data.

Through bidirectional data synthesis, we construct PIC-400K dataset. However, we need extra filtering processes to improve data quality as the dataset is still suffering from noise.

3.1.2. Multi-dimensional Perception Data Filter

Previous studies [2, 8] have shown that MLLMs have limited capability in recognizing fine-grained details in images. Instead of directly feeding image pairs into the MLLMs for filtering, we establish a reliable system to achieve more accurate and efficient data filtering. Specifically, we divide the filtering process into three levels based on granularity. **Firstly**, we segment the subjects from data pairs and utilize CLIP-I [24] and DINO [3] scores s_v to filter out images with significantly lower consistency. **Subsequently**, we pass two subjects' images through MLLMs (e.g., GPT-

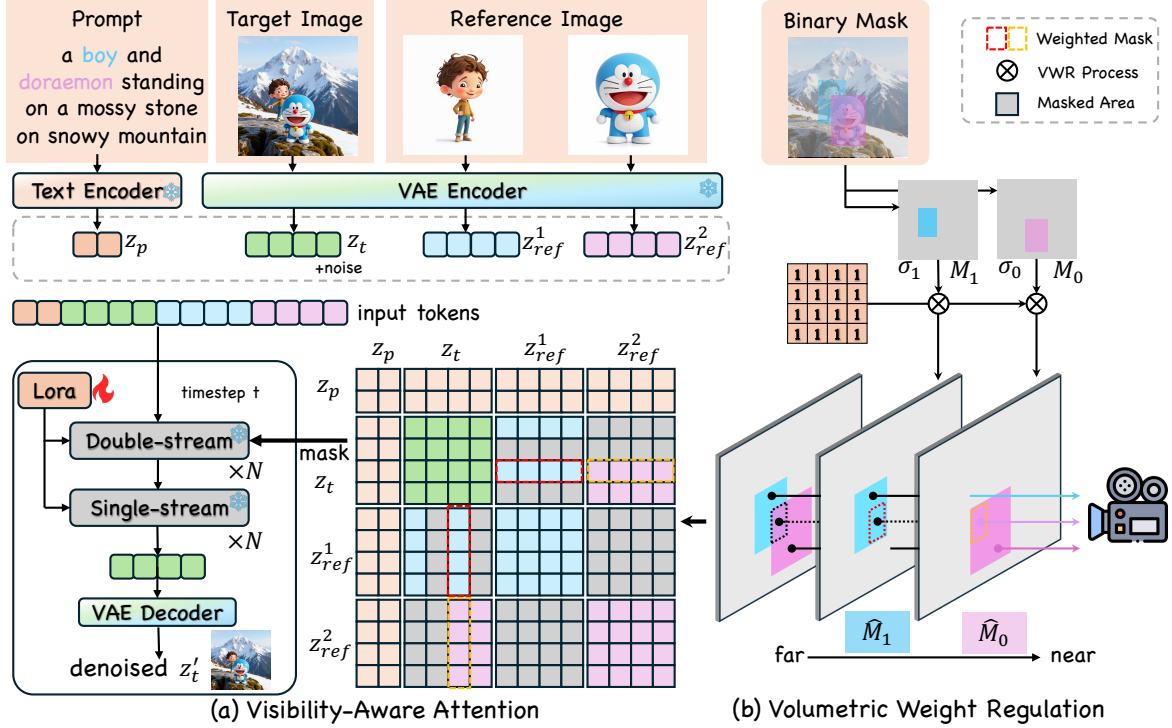


Figure 3. The overall framework of PositionIC. (a) Reference images and prompts are encoded and concatenated with the latent embeddings z_t , then the whole token sequence is passed to DiT. Each reference image z_{ref}^i is only visible for the specific area of latent noise z_t in the attention map. (b) The objects’ binary mask and the semantic density σ are used by VWR to calculate the weighted mask. The dashed boxes in the ray diagram represent the overlapping regions, where the same colors correspond to the weights in the mask.

40), which directly gives a similarity score s_{vlm} based on shape, color and so on. **Lastly**, we employ Describe Anything Model (DAM) [19], a description expert to obtain detailed textual descriptions for each subject. Given these textual description pairs, we instruct GPT-4o as a judge to autonomously select comparative features (e.g., color, shape) and assign multi-dimensional similarity scores s_{ds} .

Then we calculate the ranking separately and average them for each image pair to obtain final ranks:

$$rank = avg(r(s_v), r(s_{vlm}), r(s_{ds})), \quad (1)$$

where $r(\cdot)$ denotes rank. With a lower rank indicating a higher subject similarity.

We apply the filter on PIC-400K to rank the pairs and filter out inconsistent pairs. The filtered dataset PIC-98K consists of 44k single-subject pairs and 54k multi-subject pairs. More examples of our PIC-98K are depicted in the appendix.

3.2. PositionIC

When extending text-to-image models to image-to-image tasks, the fidelity of the generated object largely depends on the magnitude of the attention between the corresponding regions in the target image and the reference image. We

refer to this as attention accumulation. As shown in Figure 3, the attention map can be divided into four areas: text-text self attention, image-image self attention, text-image and image-text cross attention. If extending to single or multi-subject custom generation via concatenating method like [15, 28, 35, 41], the attention map will expand to nearly three times its original size, making it harder for the model to focus on the corresponding regions.

To achieve effective attention accumulation, we propose **Visibility-Aware Attention**, which utilizes volume rendering (VR) to explicitly define the area that can be focused on for each reference image. Previous works [4, 40–42] explore the effort of restricting the attention horizon between special words and noise, we extend it to subject-driven generation task to unlock the positional control ability of diffusion transformers (DiT). The overall mechanism is shown in Figure 3.

3.2.1. Volume Rendering (VR)

The weighted mask utilizes VR [13] to handle the occlusion relationships between individual objects. Similar to NeRF [20], the expected color $C(r)$ observed by the camera along the distance from the far bound t_f to the near bound



Figure 4. Qualitative comparison of single-subject generation with different methods on DreamBench.



Figure 5. Qualitative comparison of multi-subject generation with different methods on DreamBench. We adopt a fixed bounding box (e.g., bottom left and bottom right) for generation.

t_n is:

$$\begin{aligned}
 C(r) &= \int_{t_n}^{t_f} T(t)\sigma(r(t))c(r(t), d)dt, \\
 T(t) &= \exp\left(-\int_{t_n}^t \sigma(r(s))ds\right)
 \end{aligned} \tag{2}$$

where the camera ray $r(t) = o + td$, $\sigma(x)$ is volume density. We utilize the quadrature rule to obtain a discrete estimate of $C(r)$:

$$\begin{aligned}
 \hat{C}(r) &= \sum_{i=1}^N T_i(1 - \exp(-\sigma_i\delta_i))c_i, \\
 T_i &= \exp\left(-\sum_{j=1}^{i-1} \sigma_j\delta_j\right)
 \end{aligned} \tag{3}$$

where N denotes the spatial resolution for the distance range from near to far bounds. δ_i is the distance between adjacent samples.

3.2.2. Volumetric Weight Regulation

Similar to the 3D rendering process, controlling the generation position of individual objects on a 2D canvas can be viewed as a composite image captured by an orthographic virtual camera. To precisely distinguish the occlusion relationships between objects, we leverage VR to modulate a physically plausible semantic mask. Given the foreground mask M_i and the sample distance δ , the volumetric weight \hat{M}_n can be formulate as:

$$\hat{M}_n = \exp\left(-\sum_{j=1}^{n-1} \sigma_j\delta\right)(1 - \exp(-\sigma_n\delta))M_n\hat{M}_{n-1} \tag{4}$$

unlike in Eq. (3), \hat{M}_n is defined as the volumetric weight for each distance level, which is utilized to represent the degree of attention the image pays to each region of the reference image during attention calculation. Specifically, we utilize a semantic density σ_i instead of the volume density to represent the semantic interaction between objects. Setting of σ_i can be found in appendix.

3.2.3. Visibility-Aware Attention

As shown in Figure 3, we first encode the reference images I_r^i to the latent space via VAE $\epsilon(\cdot)$. Encoded results z_{ref} are then concatenated with noise latents z_t and text embedding z_p . This process can be formulated as:

$$\begin{aligned} z_{ref} &= [\epsilon(I_r^1), \epsilon(I_r^2), \dots, \epsilon(I_r^N)], \\ z &= \text{Concatenate}(z_p, z_t, z_{ref}), \end{aligned} \quad (5)$$

where N is the number of reference images and z denotes the input tokens to the DiT model.

Since the global text prompt contains information about the entire image, generating a reference object in a specific region requires focused and singular attention. They only need to pay attention to the corresponding region while ignoring other irrelevant tokens. Therefore, we use a VWR-based attention mask, which we call visibility-aware attention(VAA), to shield the regions that each token should not directly focus on. As shown in Figure 3, each reference image z_{ref} has a restricted attention horizon, which blocks the attention between itself and other reference images. Moreover, only the area within the bounding box in the noise is visible for the specific reference image. The mechanism of VAA mask M can be formulated as:

$$\begin{aligned} M(z_{ref}^i, z_{ref}^j) &= 0, i \neq j, \\ M(z_{ref}^i, z_t^n) &= \hat{M}_i, \\ M(\text{other}) &= 1, \end{aligned} \quad (6)$$

where \hat{M}_i is volumetric weight of i^{th} reference subject. Thus, the computation of attention is derived as:

$$\text{Attention} = \text{Softmax}\left(\frac{QK^T}{\sqrt{d}} + \log M\right) \cdot V \quad (7)$$

3.3. PositionIC-Bench

Most existing customized image evaluation (e.g., DreamBench) lacks explicit spatial position annotations. Thus, there is no universal data benchmark for evaluating subject-driven methods with position control. To address this gap, we propose PositionIC-Bench, a benchmark to evaluate subject consistency and position accuracy simultaneously.

We manually select 252 single-subject samples and 296 multi-subject samples in the benchmark, where the object bounding boxes conform to standard proportions and include challenging positional relationships.

4. Experiments

4.1. Implementations

4.1.1. Training Detail

Following UNO, we first initialize the model using FLUX.1 dev and apply UnoPE to extend the position embedding

of the reference images to the non-overlapping area diagonally. We train a LoRA at the rank of 512 on 8 NVIDIA A100 GPUs and set the total batch size of 128. The learning rate is set to 10^{-5} with cosine warm up. In the first stage, we train the single-subject model on 44k single-subject pairs for 10k steps. We then continue our training on 54k multi-subject pairs for 8k steps, which extends the multi-subject generation capability to the model obtained in the first stage.

Method	CLIP-I \uparrow	CLIP-T \uparrow	DINO \uparrow
Dreambooth	0.776	0.215	0.679
BLIP-Diffusion	0.787	0.234	0.742
ELITE	0.803	0.235	0.723
SSR-Encoder	0.797	0.206	0.725
RealCustom	0.783	0.242	0.765
MS-Diffusion	0.808	0.242	0.791
OmniGen	0.791	0.267	0.751
DreamO	0.835	0.258	0.802
OminiControl	0.805	<u>0.268</u>	0.735
UNO	<u>0.840</u>	0.253	<u>0.814</u>
PositionIC(<i>Ours</i>)	0.846	0.269	0.823

Table 1. Evaluation on DreamBench for single-subject driven generation. The **bold** value is the highest and the underlined value is the second.

Method	CLIP-I \uparrow	CLIP-T \uparrow	DINO \uparrow
BLIP-Diffusion	0.703	0.212	0.541
MIP-Adapter	0.752	0.254	0.657
MS-Diffusion	0.772	0.261	0.683
DreamO	0.779	0.273	0.698
UNO	<u>0.781</u>	<u>0.279</u>	<u>0.707</u>
OmniGen	0.749	0.291	0.668
PositionIC(<i>Ours</i>)	0.819	<u>0.279</u>	0.771

Table 2. Evaluation on DreamBench for multi-subject driven generation.

4.1.2. Evaluation Metrics

For subject-generation tasks, we evaluate subject similarity using CLIP-I, DINO-I on Dreambench [26]. For text fidelity, we calculate CLIP-T scores, which measure cosine similarity between the text embedding and image embedding from CLIP.

For the position-guided task, we evaluate different methods on our proposed PositionIC-Bench. We use Vision-R1 [11] to determine the bounding box of the subject and calculate mIoU and AP scores with the label.

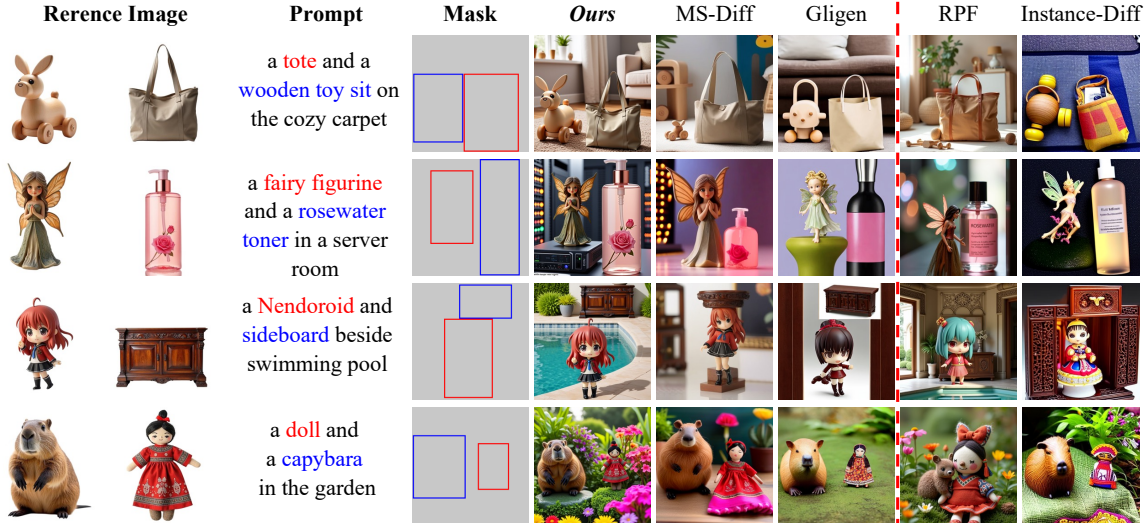


Figure 6. Qualitative comparison of position control generation with different methods on PositionIC-Bench. MS-Diff and RPF denote MS-Diffusion and Regional Prompting Flux respectively. MS-Diff and Gligen are existing position-controllable customization methods; RPF and Instance-Diff are position-only controllable methods.

Method	Single-Subject			Multi-Subject	
	IoU \uparrow	$AP \uparrow / AP_{50} \uparrow / AP_{70} \uparrow$	mIoU \uparrow	$AP \uparrow / AP_{50} \uparrow / AP_{70} \uparrow$	
RPF [4]	0.341	0.015 / 0.063 / 0.007	0.369	0.070 / 0.002 / 0.011	
MS-Diffusion [33]	0.501	0.097 / 0.329 / 0.075	0.421	0.028 / 0.146 / 0.005	
Instance-Diffusion [32]	0.789	0.593 / 0.683 / 0.632	0.799	0.497 / 0.699 / 0.546	
Gligen [18]	<u>0.808</u>	0.632 / 0.865 / 0.811	<u>0.825</u>	<u>0.628 / 0.858 / 0.811</u>	
PositionIC(<i>Ours</i>)	0.828	<u>0.628 / 0.904 / 0.761</u>	0.860	0.701 / 0.939 / 0.853	

Table 3. Quantitative results of controllable spacial generation on PositionIC-Bench.

4.2. Qualitative Result

We visualize the comparison results with the current state-of-the-art methods in Figure 4. Overall, our method surpasses all current methods in terms of visual effects. It can be seen that our method can still effectively follow the prompt while maintaining subject consistency, demonstrating higher text fidelity. Other methods either fail to follow complex instructions or cannot maintain consistency. (e.g., UNO and DreamO cannot reproduce the dog face, while SSR-Encoder fails to add the Santa hat.) The results of the third row also reveal that PositionIC has a great capability on patterns and text. Furthermore, PositionIC consistently produces images with a higher degree of naturalness and visual plausibility. More examples can be found in Appendix.

Figure 5 shows the comparison of multi-subject generation. To control variables, the images generated by our method adopt a fixed bounding box (e.g., bottom left and bottom right). In a more difficult multi-subject scenario, PositionIC can still maintain high subject similarity and fol-

low the given text prompt, whereas results from most other methods fail to preserve consistency for each subject and even ignore certain subjects.

We further evaluate the positional control capability of existing methods on PositionIC-Bench via randomly generating the bounding boxes. As shown in Figure 6, PositionIC accurately generates subjects that fully occupy the bounding box without damaging their features. More importantly, our flux-based approach significantly outperforms others in terms of image aesthetic quality and the logical coherence of multi-subject compositions.

4.3. Quantitative Evaluations

4.3.1. Subject-driven Analyses

Specifically, we discover that different object sizes can lead to inaccurate scores, which will be detailed in Appendix.

We compare our proposed PositionIC with several leading methods on DreamBench for both single-subject and multi-subject. As presented in Table 1 and Table 2, Po-

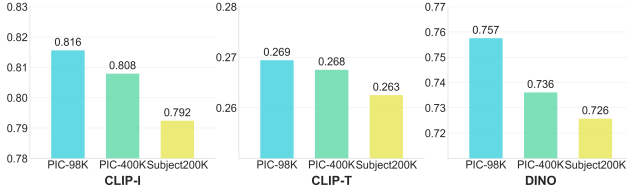


Figure 7. Ablation study of data filter. We train our model on PIC-98K, PIC-400K and Subject200K respectively.

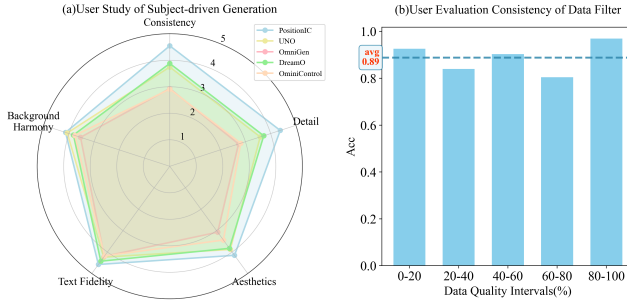


Figure 8. User study for subject-driven generation and data filter. (a) User evaluation on Dreambench. (b) Filtering consistency of our data filter compared with human in different data quality intervals (from good to bad).

sitionIC achieves the highest scores on both CLIP-I and DINO of 0.846 and 0.823 on single-subject, 0.819 and 0.771 on multi-subject, respectively. PositionIC also has competitive CLIP-T compared to existing methods. The evaluation results indicate that PositionIC has remarkable performance on subject consistency and text fidelity.

4.3.2. Controllable Spatial Generation

Table 3 presents the results of spatial control evaluation. PositionIC achieves superior performance in both single-subject and multi-subject position control. For single-subject position control, PositionIC has the highest IoU of 0.828 across all methods and has competitive AP scores compared with Gligen. For multi-subject evaluation, PositionIC achieves the highest scores in both AP and IoU scores, demonstrating a significant advantage over existing methods.

4.3.3. User Study

We invite evaluators for an extensive user study. For subject-driven generation, we randomly selected 500 images from the results on DreamBench for manual evaluation. Six users scored the results from five dimensions, each ranging from 0 to 5, and the average score was taken. The result presented in Figure 8 (a) shows that our method reaches the highest capability to preserve image features and details while maintaining competitive text adherence.

To evaluate the consistency between human annotators and the data filter in BMPDS, we use percentage agreement metric (denoted as Acc.), comparing the filter’s output against human-generated annotations. As shown in Figure 8

(b), our filter has an average consistency of 0.89 with human annotators.

4.4. Ablation Study

In this section we show the ablation study of our key modules, including data quality and Volumetric Weight Regulation(VWR). More ablation results are presented in the appendix.

4.4.1. Impact of data filter.

Results in Figure 7 illustrate the advanced fidelity of BMPDS. We directly trained with PIC-98K, PIC-400K and the Subject200K dataset without injecting position control information. PIC-400K achieves significantly higher scores than Subject200K, and the filtered data PIC-98K achieves the highest scores overall, which demonstrates the remarkable efficiency of our data synthesis and filtering pipeline.

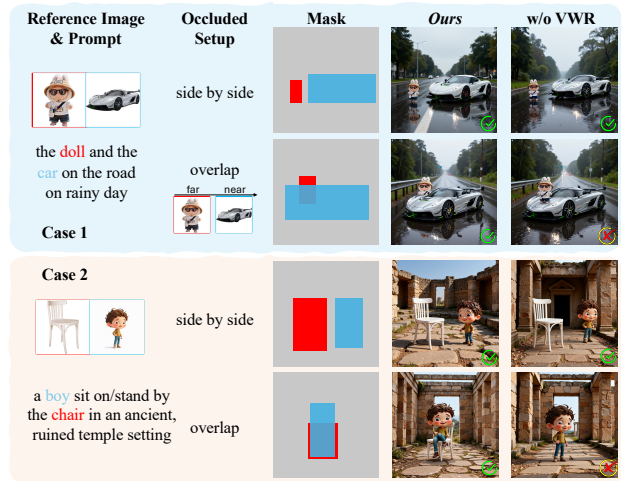


Figure 9. Impact of VWR. In the presence of overlaps, VWR is capable of correctly handling the spatial relationships between objects. We set the attention value in overlap region as 1 to disable VWR.

4.4.2. Abation results of Volumetric Weight Regulation(VWR)

As shown in Fig. 9, in Case 1 overlap setting, the doll is instructed to be placed behind the sports car. However, the model fails to correctly understand their spatial relationship without VWR. In Case 2, VWR is able to prevent the generation of missing objects caused by concept confusion, even when multiple objects overlap.

5. Conclusion

In this work, we present PositionIC, an innovative framework capable of customizing multiple subjects with precise position control. PositionIC decouples layout signal from subject feature without introducing additional parameters

and training cost. Additionally, we carefully design an automatic data curation framework to obtain high-fidelity paired data. We adopt bidirectional generation and present a multi-dimensional perception filter to improve object consistency in acquired data. Extensive experiments demonstrate that PositionIC performs high-quality generation in both single-subject and multi-subject consistency, as well as in controllable subject positioning. We hope our work can advance the development of controllable image customization.

References

- [1] Omer Bar-Tal, Lior Yariv, Yaron Lipman, and Tali Dekel. Multidiffusion: fusing diffusion paths for controlled image generation. In *Proceedings of the 40th International Conference on Machine Learning*. JMLR.org, 2023. 2
- [2] Yue Cao, Yangzhou Liu, Zhe Chen, Guangchen Shi, Wenhai Wang, Danhuai Zhao, and Tong Lu. Mmfuser: Multimodal multi-layer feature fuser for fine-grained vision-language understanding. *arXiv preprint arXiv:2410.11829*, 2024. 3
- [3] Mathilde Caron, Hugo Touvron, Ishan Misra, Hervé Jégou, Julien Mairal, Piotr Bojanowski, and Armand Joulin. Emerging properties in self-supervised vision transformers. In *Proceedings of the IEEE/CVF international conference on computer vision*, pages 9650–9660, 2021. 3
- [4] Anthony Chen, Jianjin Xu, Wenzhao Zheng, Gaole Dai, Yida Wang, Renrui Zhang, Haofan Wang, and Shanghang Zhang. Training-free regional prompting for diffusion transformers. *arXiv preprint arXiv:2411.02395*, 2024. 2, 4, 7
- [5] Patrick Esser, Sumith Kulal, Andreas Blattmann, Rahim Entezari, Jonas Müller, Harry Saini, Yam Levi, Dominik Lorenz, Axel Sauer, Frederic Boesel, Dustin Podell, Tim Dockhorn, Zion English, Kyle Lacey, Alex Goodwin, Yan-nik Marek, and Robin Rombach. Scaling rectified flow transformers for high-resolution image synthesis, 2024. 1
- [6] Haoran Feng, Zehuan Huang, Lin Li, Hairong Lv, and Lu Sheng. Personalize anything for free with diffusion transformer. *arXiv preprint arXiv:2503.12590*, 2025. 2
- [7] Tianyang Han, Qing Lian, Rui Pan, Renjie Pi, Jipeng Zhang, Shizhe Diao, Yong Lin, and Tong Zhang. The instinctive bias: Spurious images lead to illusion in mllms. *arXiv preprint arXiv:2402.03757*, 2024. 2
- [8] Hulingxiao He, Geng Li, Zijun Geng, Jinglin Xu, and Yuxin Peng. Analyzing and boosting the power of fine-grained visual recognition for multi-modal large language models. *arXiv preprint arXiv:2501.15140*, 2025. 3
- [9] Edward J Hu, Yelong Shen, Phillip Wallis, Zeyuan Allen-Zhu, Yuanzhi Li, Shean Wang, Lu Wang, Weizhu Chen, et al. Lora: Low-rank adaptation of large language models. *ICLR*, 1(2):3, 2022. 2
- [10] Mengqi Huang, Zhendong Mao, Mingcong Liu, Qian He, and Yongdong Zhang. Realcustom: Narrowing real text word for real-time open-domain text-to-image customization. In *Proceedings of the IEEE/CVF Conference on Computer Vision and Pattern Recognition*, pages 7476–7485, 2024. 2
- [11] Wenxuan Huang, Bohan Jia, Zijie Zhai, Shaosheng Cao, Zheyu Ye, Fei Zhao, Zhe Xu, Yao Hu, and Shaohui Lin. Vision-r1: Incentivizing reasoning capability in multimodal large language models. *arXiv preprint arXiv:2503.06749*, 2025. 6
- [12] Álvaro Barbero Jiménez. Mixture of diffusers for scene composition and high resolution image generation. *arXiv preprint arXiv:2302.02412*, 2023. 2
- [13] James T. Kajiya and Brian P Von Herzen. Ray tracing volume densities. In *Proceedings of the 11th Annual Conference on Computer Graphics and Interactive Techniques*, page 165–174, New York, NY, USA, 1984. Association for Computing Machinery. 4
- [14] Black Forest Labs. Flux. <https://github.com/black-forest-labs/flux>, 2024. 1
- [15] Black Forest Labs, Stephen Batifol, Andreas Blattmann, Frederic Boesel, Saksham Consul, Cyril Diagne, Tim Dockhorn, Jack English, Zion English, Patrick Esser, Sumith Kulal, Kyle Lacey, Yam Levi, Cheng Li, Dominik Lorenz, Jonas Müller, Dustin Podell, Robin Rombach, Harry Saini, Axel Sauer, and Luke Smith. Flux.1 kontext: Flow matching for in-context image generation and editing in latent space, 2025. 2, 4
- [16] Dongxu Li, Junnan Li, and Steven Hoi. Blip-diffusion: Pre-trained subject representation for controllable text-to-image generation and editing. *Advances in Neural Information Processing Systems*, 36:30146–30166, 2023. 2
- [17] Daiqing Li, Aleks Kamko, Ehsan Akhgari, Ali Sabet, Linmiao Xu, and Suhail Doshi. Playground v2. 5: Three insights towards enhancing aesthetic quality in text-to-image generation. *arXiv preprint arXiv:2402.17245*, 2024. 1
- [18] Yuheng Li, Haotian Liu, Qingyang Wu, Fangzhou Mu, Jianwei Yang, Jianfeng Gao, Chunyuan Li, and Yong Jae Lee. Gligen: Open-set grounded text-to-image generation. *CVPR*, 2023. 2, 7
- [19] Long Lian, Yifan Ding, Yunhao Ge, Sifei Liu, Hanzi Mao, Boyi Li, Marco Pavone, Ming-Yu Liu, Trevor Darrell, Adam Yala, and Yin Cui. Describe anything: Detailed localized image and video captioning. *arXiv preprint arXiv:2504.16072*, 2025. 4
- [20] Ben Mildenhall, Pratul P. Srinivasan, Matthew Tancik, Jonathan T. Barron, Ravi Ramamoorthi, and Ren Ng. Nerf: representing scenes as neural radiance fields for view synthesis. *Commun. ACM*, 65(1):99–106, 2021. 2, 4
- [21] Chong Mou, Yanze Wu, Wenxu Wu, Zinan Guo, Pengze Zhang, Yufeng Cheng, Yiming Luo, Fei Ding, Shiwen Zhang, Xinghui Li, Mengtian Li, Mingcong Liu, Yi Zhang, Shaojin Wu, Songtao Zhao, Jian Zhang, Qian He, and Xinglong Wu. Dreamo: A unified framework for image customization, 2025. 1, 2
- [22] Renjie Pi, Tianyang Han, Wei Xiong, Jipeng Zhang, Runtao Liu, Rui Pan, and Tong Zhang. Strengthening multi-modal large language model with bootstrapped preference optimization. In *European Conference on Computer Vision*, pages 382–398. Springer, 2024. 2
- [23] Dustin Podell, Zion English, Kyle Lacey, Andreas Blattmann, Tim Dockhorn, Jonas Müller, Joe Penna, and

- Robin Rombach. Sdxl: Improving latent diffusion models for high-resolution image synthesis. *arXiv preprint arXiv:2307.01952*, 2023. 1
- [24] Alec Radford, Jong Wook Kim, Chris Hallacy, Aditya Ramesh, Gabriel Goh, Sandhini Agarwal, Girish Sastry, Amanda Askell, Pamela Mishkin, Jack Clark, et al. Learning transferable visual models from natural language supervision. In *International conference on machine learning*, pages 8748–8763. PMLR, 2021. 3
- [25] Robin Rombach, Andreas Blattmann, Dominik Lorenz, Patrick Esser, and Björn Ommer. High-resolution image synthesis with latent diffusion models. In *Proceedings of the IEEE/CVF conference on computer vision and pattern recognition*, pages 10684–10695, 2022. 1
- [26] Nataniel Ruiz, Yuanzhen Li, Varun Jampani, Yael Pritch, Michael Rubinstein, and Kfir Aberman. Dreambooth: Fine tuning text-to-image diffusion models for subject-driven generation. In *Proceedings of the IEEE/CVF Conference on Computer Vision and Pattern Recognition*, pages 22500–22510, 2023. 2, 6
- [27] Hengyu Shi, Junhao Su, Huansheng Ning, Xiaoming Wei, and Jialin Gao. Layoutcot: Unleashing the deep reasoning potential of large language models for layout generation. *arXiv preprint arXiv:2504.10829*, 2025. 2
- [28] Zhenxiong Tan, Songhua Liu, Xingyi Yang, Qiaochu Xue, and Xinchao Wang. Ominicontrol: Minimal and universal control for diffusion transformer. *arXiv preprint arXiv:2411.15098*, 2024. 1, 2, 3, 4
- [29] Zhenxiong Tan, Qiaochu Xue, Xingyi Yang, Songhua Liu, and Xinchao Wang. Ominicontrol2: Efficient conditioning for diffusion transformers. *arXiv preprint arXiv:2503.08280*, 2025. 2
- [30] Haoxuan Wang, Jinlong Peng, Qingdong He, Hao Yang, Ying Jin, Jiafu Wu, Xiaobin Hu, Yanjie Pan, Zhenye Gan, Mingmin Chi, et al. Unicombine: Unified multi-conditional combination with diffusion transformer. *arXiv preprint arXiv:2503.09277*, 2025. 1
- [31] Ruichen Wang, Zekang Chen, Chen Chen, Jian Ma, Haonan Lu, and Xiaodong Lin. Compositional text-to-image synthesis with attention map control of diffusion models. In *Proceedings of the AAAI Conference on Artificial Intelligence*, pages 5544–5552, 2024. 2
- [32] Xudong Wang, Trevor Darrell, Sai Saketh Rambhatla, Rohit Girdhar, and Ishan Misra. Instancediffusion: Instance-level control for image generation. In *Proceedings of the IEEE/CVF conference on computer vision and pattern recognition*, pages 6232–6242, 2024. 2, 7
- [33] Xierui Wang, Siming Fu, Qihan Huang, Wanggui He, and Hao Jiang. Ms-diffusion: Multi-subject zero-shot image personalization with layout guidance. *arXiv preprint arXiv:2406.07209*, 2024. 2, 7
- [34] Yuxiang Wei, Yabo Zhang, Zhilong Ji, Jinfeng Bai, Lei Zhang, and Wangmeng Zuo. Elite: Encoding visual concepts into textual embeddings for customized text-to-image generation. In *Proceedings of the IEEE/CVF International Conference on Computer Vision*, pages 15943–15953, 2023. 2
- [35] Shaojin Wu, Mengqi Huang, Wenxu Wu, Yufeng Cheng, Fei Ding, and Qian He. Less-to-more generalization: Unlocking more controllability by in-context generation. *arXiv preprint arXiv:2504.02160*, 2025. 1, 2, 4
- [36] Guangxuan Xiao, Tianwei Yin, William T Freeman, Frédo Durand, and Song Han. Fastcomposer: Tuning-free multi-subject image generation with localized attention. *arXiv preprint arXiv:2305.10431*, 2023. 2
- [37] Shitao Xiao, Yueze Wang, Junjie Zhou, Huaying Yuan, Xingrun Xing, Ruiran Yan, Chaofan Li, Shuting Wang, Tiejun Huang, and Zheng Liu. Omnigen: Unified image generation. In *Proceedings of the Computer Vision and Pattern Recognition Conference*, pages 13294–13304, 2025. 2
- [38] Zhexiao Xiong, Wei Xiong, Jing Shi, He Zhang, Yizhi Song, and Nathan Jacobs. Groundingbooth: Grounding text-to-image customization, 2025. 2
- [39] Hu Ye, Jun Zhang, Sibao Liu, Xiao Han, and Wei Yang. Ip-adapt: Text compatible image prompt adapter for text-to-image diffusion models. *arXiv preprint arXiv:2308.06721*, 2023. 2
- [40] Xiaohang Zhan and Dingming Liu. Larender: Training-free occlusion control in image generation via latent rendering, 2025. 2, 4
- [41] Hong Zhang, Zhongjie Duan, Xingjun Wang, Yingda Chen, and Yu Zhang. Eligen: Entity-level controlled image generation with regional attention, 2025. 4
- [42] Hui Zhang, Dexiang Hong, Maoke Yang, Yutao Cheng, Zhao Zhang, Jie Shao, Xinglong Wu, Zuxuan Wu, and Yu-Gang Jiang. Creatidesign: A unified multi-conditional diffusion transformer for creative graphic design, 2025. 4

PositionIC: Unified Position and Identity Consistency for Image Customization

Supplementary Material

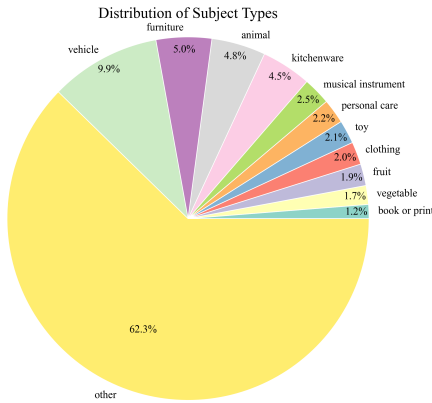


Figure 10. Category distribution of PIC-98K.



Figure 11. Showcases of PositionIC-Bench.

In Section 6, we give a detailed description of our data synthesis and filtering pipeline: Bidirectional Multi-dimensional Perception Data Synthesis (BMPDS). We further present a selection of example images. Section 7 introduces the PositionIC-Bench we use for position evaluation.

Section 8,9 and 10 provide a detailed discussion of specific experimental setups and additional ablation studies. Furthermore, more example demonstrations can be found in Figure 12.

6. Bidirectional Multi-dimensional Perception Data Synthesis

6.1. Detailed Instruction of GPT-4o

As shown in Figure 15, the message given to GPT-4o consists of **Instruction**, **Evaluation Metric** and **Response**. In the part of **Instruction**, we have defined the input format and evaluation metric dimensions, and required GPT-4o to select no fewer than three features for scoring based on the content of textual description. In the next part of **Evaluation Metric**, we detail the metric standard and provide GPT-4o examples to evaluate. There are 6 levels, ranging from 0 to 5, representing the similarity between two descriptions regarding the same feature. After that, we prompt GPT-4o to return a dictionary in JSON format containing the subject types and the scores for each feature. If there is no similarity between the two descriptions, the subject is set to "none", indicating that the final score is 0.

Due to the substantial differences in textual descriptions between subjects, it is not feasible to predetermine the feature categories for evaluation. Therefore, we allow the LLMs to select at least three features and assign individual

scores to each. The final score is calculated as the average of all feature scores. For descriptions with significant discrepancies, the LLMs are permitted to assign a score of zero to the samples.

Figure 17 demonstrates the samples of Multi-dimensional Perception Data Filter. We have highlighted the correlated features in the description. In the first sample, the teddy bear share the same physical characteristics except for their posture, hence earning the highest appearance score and slightly lower posture score. In the second sample, the deer is missing antlers, which resulted in the lowest score on the "antler" feature.

6.2. Details of PIC-98K Dataset

We propose PIC-400K utilizing our Bidirectional Multi-dimensional Perception Data Synthesis, an automatic and effective high-consistency data synthesis pipeline. Samples of the filtered data PIC-98K are shown in the Figure 16. BMPDS can synthesize high-fidelity multi-subject images while maintaining high resolution. Against previous works, the position of subjects is controllable and it is randomly placed to train the position control capability of PositionIC.

There are over 9000 subject descriptions in PIC-98K, including multiple categories such as fruits, animals, and transportation vehicles, which basically cover common objects. The distribution of subjects is shown in Figure 10, vehicles, furniture, animal, and kitchenware constitute a significant proportion, with most difficult-to-classify subjects categorized as "other".

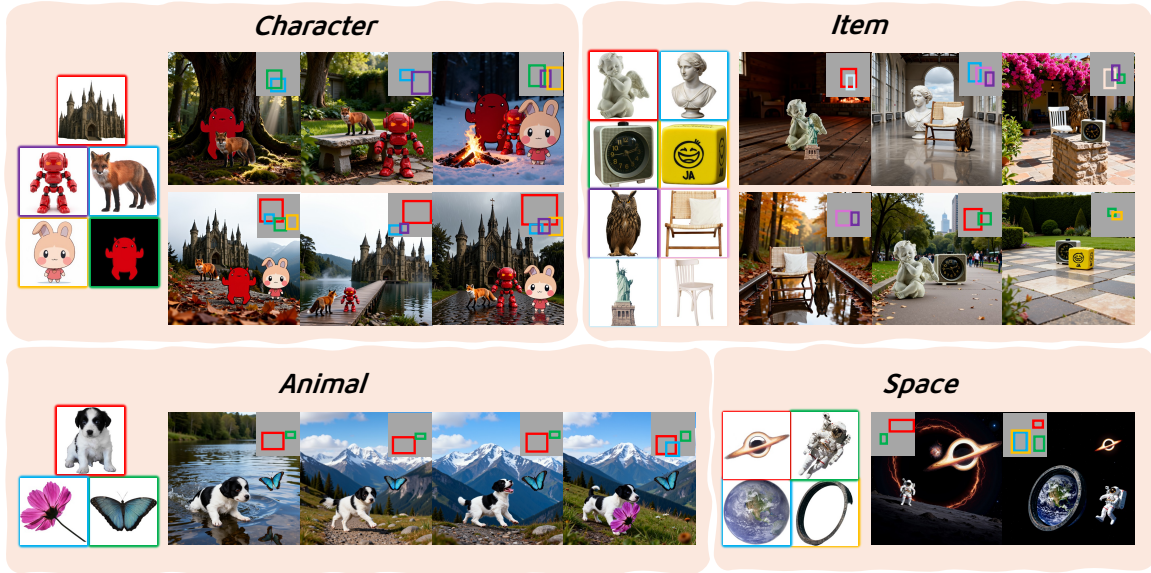


Figure 12. More results about PositionIC.

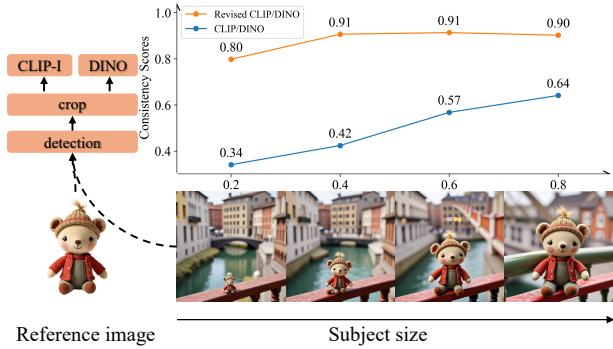


Figure 13. Inaccuracy of directly using CLIP-I and DINO. The revised score is less affected by the size of the subject which can reflect the subject consistency more authentically.

7. PositionIC-Bench

We manually select 252 single-subject samples and 296 multi-subject samples in the benchmark, where the object bounding boxes conform to standard proportions and include challenging positional relationships. We show some samples of PositionIC-Bench in Figure 11. Our bench includes various subjects such as furniture, animals, plants, and portraits. Not limited to conventional object placement, PositionIC-Bench’s bounding boxes have more complex spatial relationships where objects are placed on different planes. At the same time, the bounding boxes of smaller objects is appropriately enlarged to obtain more accurate evaluation scores.

8. Training Details and Result

8.1. Setting of Training

The value of the semantic density σ_i can be manually set or determined by Eq. (8). In Eq. (8), we set the semantic density to a geometric progression with a common ratio of $1 + 10\lambda$, which represents that σ_i increases incrementally from far to near to reflect the difference between foreground and background objects.

$$\sigma_i = \frac{10\lambda * (1 + 10\lambda)^i}{(1 + 10\lambda)^n - 1}, \quad (8)$$

where n is the number of reference images and $i = \{0, 1, 2, \dots, n - 1\}$ represents the object index ordered from far to near. λ is a hyperparameter used to control the variation in semantic density. A smaller value of λ results in less difference in semantic density between objects. During training, we set it to 5.

8.2. More Result

As shown in Figure 12, we downloaded several foreground images from the internet as additional visual demonstrations, covering four categories: Characters, Items, Animals, and Space. In the Characters and Items sections, PositionIC exhibits high fidelity and is capable of generating images with coherent spatial relationships. In the Animals section, we demonstrate the plausibility of object interactions under different prompts. In the Space section, PositionIC is able to achieve good results even for difficult examples (e.g., generating a planetary ring surrounding the Earth).

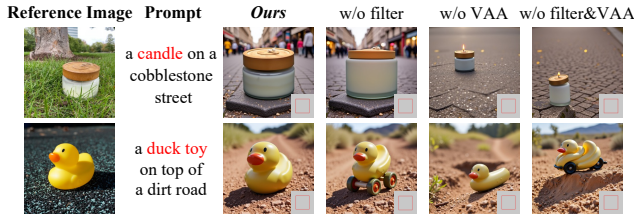


Figure 14. Qualitative results of ablation study. Visibility-Aware Attention(VAA) and our filter pipeline are capable of effective position control and consistent customization.

9. Revised Evaluation Metric

In this section, we elaborate on the calculation methods for our evaluation metrics. As shown in Figure 13, directly using the entire image to compute the CLIP or DINO metrics is unreasonable, as both CLIP and DINO compute the similarity of global image features. To avoid the sensitivity, we crop the subject from original image as source images for evaluation.

10. More Ablation Study

In this section, we conduct more detailed ablation studies, including ablations on the data filter and Visibility-Aware Attention(VAA).

10.1. Impact of Visibility-Aware Attention

As shown in Figure 4, CLIP-I and DINO scores significantly drop when training without VAA. We infer that incorporating a attention mask allows the model to focus more effectively on features in a smaller region rather than globally, which accelerates the convergence and improves the consistency.

10.2. Qualitative Results

As shown in Figure 14, we visualize the effect of VAA and data filtering. It can be seen that without VAA, the model loses the ability to control position. When using unfiltered data, although the data volume is larger, the generated quality is poorer.

Method	CLIP-I \uparrow	CLIP-T \uparrow	DINO \uparrow
w/o VAA	0.784	0.269	0.686
w/ VAA	0.846	0.269	0.823

Table 4. Ablation study of VAA. Our model performs better subject fidelity on DreamBench after restricting the attention area of reference images.

Instruction

You will receive two paragraphs of text, which are detailed descriptions of two different images. The input is in the following format:

describe_1:detailed describe <end>.describe_2:detailed describe <end>.

There will be a common subject in these two images.

For example, both paragraphs describe a dog. The first paragraph is a dog swimming, and the second paragraph is a dog running.

The description given to you will include a description of the subject. You need to find the common subject in the two images based on these descriptions and determine whether the two subjects are the same. Note that you need to distinguish the same at the instance level. For example, the first dog is a normal Shiba Inu, and the second dog is a Shiba Inu with different patterns. Then the two subjects are not the same. You will score the similarity of the subject from the following dimensions:

1. The similarity of key features. Such as the dog's body shape, body proportions, species, etc.
2. Distinguish between permanent features and temporary features. For example, patterns and colors are permanent features, while wearing a hat and being dirty are temporary features. Permanent features are more reliable than temporary features.

You need to decide on at least 3 features to score, and using as many feature dimensions as possible to judge.

Evaluation criteria

The scoring criteria are:

0 points: completely different objects, such as a dog and a car

1 point: completely different, but similar, such as a dog and a cat

2 points: the same object, but not guaranteed to be the same instance, such as two dogs

3 points: the same object, and the same type, such as two corgis

4 points: almost identical objects, such as two dogs with the same pattern

5 points: completely identical objects, with almost the same text description

Response

Note that you need to judge the credibility of the feature for identifying the subject. The higher the credibility, the greater the weight of its similarity. Finally, you need to output your score in the form of a python dictionary, in the following format:

```
{{  
"subject":""," "<feature1>":5, "<feature2>":3, .....  
}}
```

You need to fill in the value corresponding to the subject with the name of the subject you identified, such as dog. If you think there is no common subject in these two text descriptions, fill in "none".\n

At the same time, replace <feature1>, <feature2>, etc. with the feature dimensions you decided.

Figure 15. Prompt template of MLLMs in Multi-dimensional Perception Data Filter.

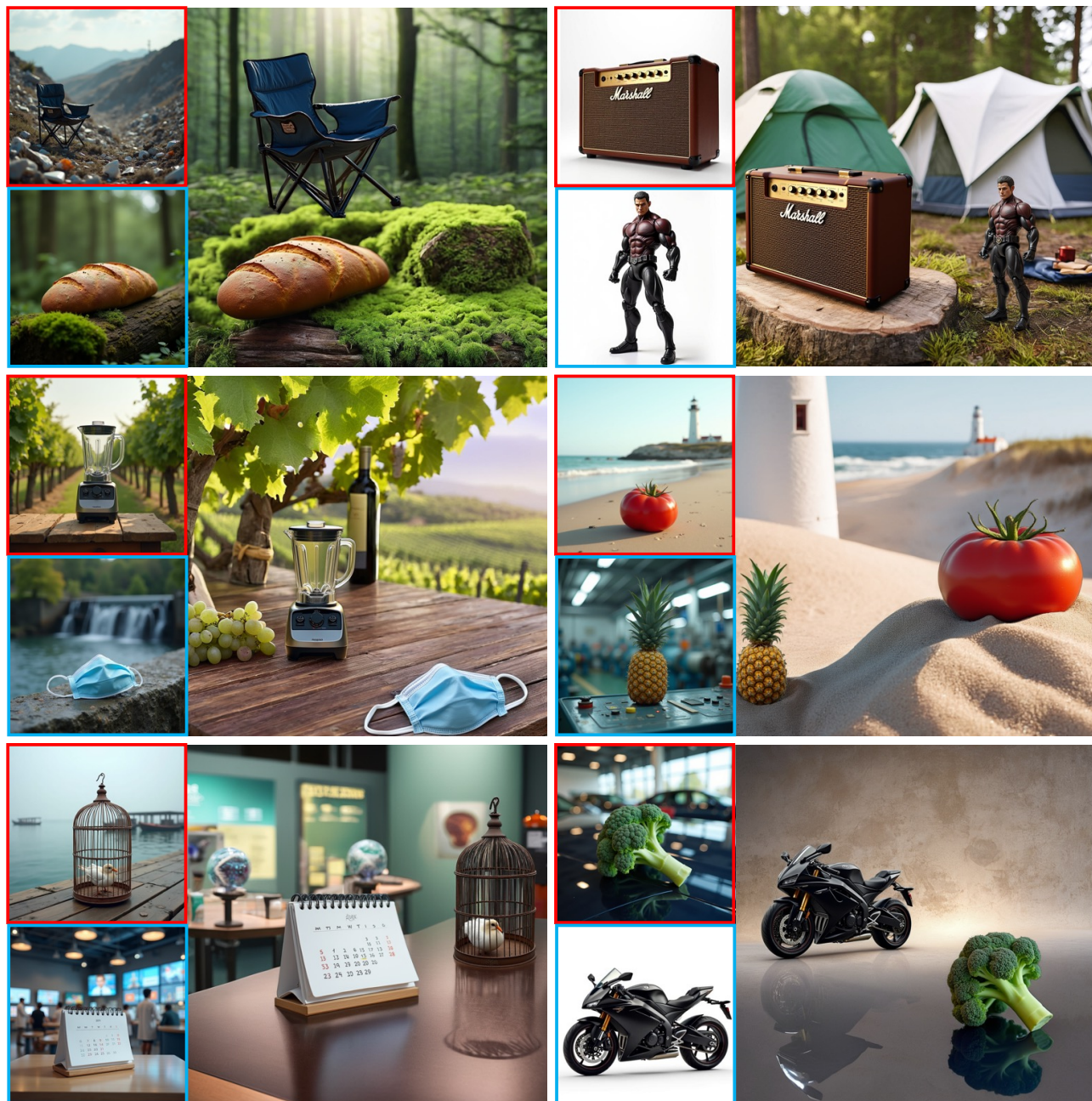


Figure 16. Showcases of PIC-98K Dataset.

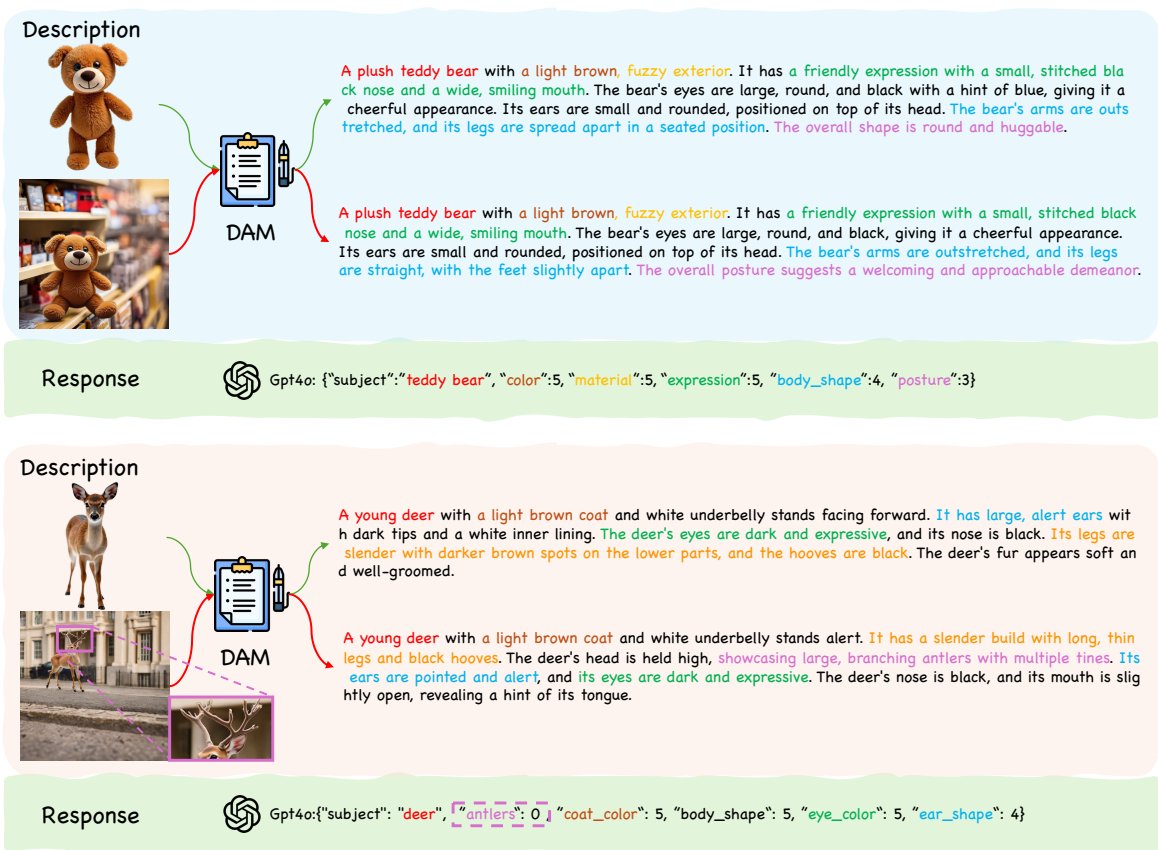


Figure 17. Examples of Multi-dimensional Perception Data Filter.